Aixin CHEN[1], Weiwei JIANG[1], Zhizhang CHEN[2], Ying Li[1]

Beihang University (1), Dalhousie University (2)

A Low-Loss Ka-Band Distributed Metal-Air-Metal MEMS Phase Shifter

***Abstract**. A 4-bit wideband distributed phase shifter has been developed for Ka-band operation. The design results show that the digital shifter has four basic phases of 11.25°, 22.5°, 45°, 90° and thus 16 kinds of phase states can be constructed from the combination of them. The simulation results also demonstrates that the insertion coefficient is better than -1.37 dB, the phase error is less than 3.983° at 30GHz, and the reflection coefficient is lower than -10dB from 25GHz to 35GHz for each state. This low-loss distributed metal-air-metal MEMS phase shifter can be well applied to phased arrays.*

***Streszczenie.** W artykule opisano 4-bitowy szerokopasmowy przesuwnik fazy zaprojektowany do pasma Ka. Przesuwnik ma cztery]główne fazy: 11.25°, 22.5°, 45°, 90° i 16 kombinacji między nimi. Błąd jest mniejszy niż 3.983° przy 30GHz. (**Szerokopasmowy przesuwnik fazy na pasmo Ka bazujący na układzie MEMS typu metal-powietrze –metal**)*

Keywords: MEMS; Phase Shifter; Low-loss.
Słowa kluczowe: MEMS, szerokopasmowy przesuwnik fazy.

Introduction

Over the past decades, RF micro-electromechanical systems (MEMS) technology has offered solutions for the implementation of novel components and systems. Concepts of Radio Frequency (RF) MEMS have been successfully applied to the development of low-loss RF switching devices and variable capacitors [1-2]. Compared with conventional switches, RF MEMS capacitive switches have demonstrated many merits, such as lower loss, lower power consumption and higher linearity [3-5]. Utilizing these switches in multi-bit phase shifters can drastically reduce loss and significantly reduce cost and weight for phased array antennas where thousands of phase shifters are mounted. Recently, researchers have reported several ways to implement multi-bit phase shifters [6-8]. A 4.5-bit distributed phase shifter based on MEMS switching devices was implemented with low insertion loss [8]. With the development of phased array antennas, higher performance is required for phase shifters. RF MEMS technology is a key approach for building low loss and size multi-bit phase shifters.

Conventional MEMS distributed phase shifter consists of a high impedance coplanar waveguide (CPW) transmission line (t-line) periodically loaded by MEMS switches. In the switch, MEMS bridge combining with central conductor covered insulator of CPW produces a shunt variable metal-insulator-metal (MIM) capacitor. By applying a control voltage to change the height of the MEMS bridges, the varactors introduce different phase velocities on the transmission. While different phase velocities are able to provide different phase differences. So we can see that the accuracies of the control voltage and the height of bridge have an impact on the performance of the phase shifter.

In this paper, a low-loss distributed MEMS 4-bit phase shifter operating at 30 GHz is proposed. It is achieved by loading two metals on sides of MEMS bridges of the CPW. The metals combining with MEMS bridge and air make up metal-air-metal (MAM) capacitors. MAM capacitors in series with MIM capacitors composite shunt capacitors in the equivalent circuit. When the MEMS bridges are in the down-state position, the MAM capacitances are much smaller than the MIM capacitances. In the series circuit, the MIM capacitances can be ignored and the MAM capacitances play an major role in the shunt capacitances. The MAM capacitances are determined by acreage of the MAM, while the shunt capacitances of conventional MEMS phase shift are decided by the height of the bridges. The acreage of the MAM is more easily to be adjusted and can be adjusted more accurately than the height of the MAM. So this design can realize the reduction of the loss and the assurance of the stability. The phase shifter with MAM capacitors proposed in this paper is better suited to Ka-band applications than conventional phase shifters.

The remainder of the paper is organized as follows. First, the principle and structure design for the unit cell of MEMS phase shifter are described. Second, analysis and simulation of the proposed 4-bit MEMS phase shifter are presented. Finally, conclusions are drawn.

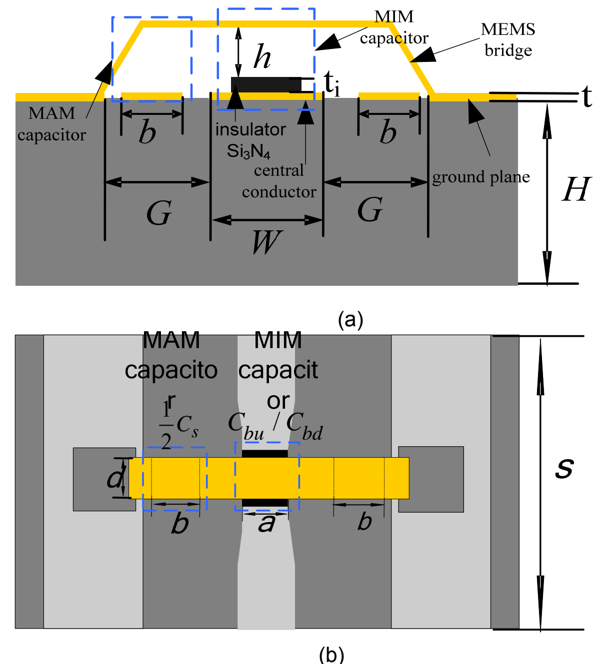

Fig. 1. Geometry of the unit cell. (a) Side view. (b) Top view.

Principle and Unit Cell Structure Design

As shown in Fig. 1, a unit cell of the MEMS phase shifter in this study includes a high-impedance CPW line loaded by the capacitive placement of a series-connected MIM capacitor and MAM capacitor. MAM capacitor is produced by adding two metals in the gap between central conductor and ground plane of the CPW. The capacitive placements equal to periodic capacitors connection on the microstrip transmission line (t-line) in parallel. There are two states of

the phase shifter: up and down. Up is the original height of the MEMS bridge while down is the state that the bridge is actuated. The two states make the phase velocity changes, thus providing a differential phase shift.

Coplanar waveguide (CPW) line periodically loaded by MIM capacitors and MAM capacitors is equivalent to add capacitive loads in the structure. It will come into being the result that the characteristic impedance is reduced. In order to reduce the reflection loss caused by impedance mismatching, the central conductor of CPW is narrowed at the place where the MEMS bridges are loaded (see Figure 1 (b)). It is equivalent to add series inductances and shunt capacitors [9, 10]. The shunt capacitors are small relative to the capacitors of the MIM and MAM, so it can be ignored in the following analysis.

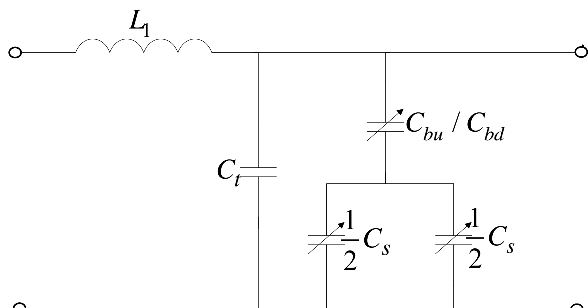

Fig. 2. Lumped model of a unit cell of the phase shifter with MEMS bridge and series MAM capacitors.

The unit cell of a CPW t-line with MEMS bridge and series MAM capacitors can be approximated as the lumped model, which is shown in Fig. 2. In this circuit, L_1 consists of two parts of L_t and L', where L_t and C_t are the inductance and capacitance of the t-line, respectively. L' is the inductance produced by the narrowed central conductor of CPW. C_t and L_t can be achieved by follows [11]:

$$C_t = \sqrt{\varepsilon_{r,eff}}\,/\,cZ_0 \tag{1}$$

$$L_t = C_t Z_0^2 \tag{2}$$

L' is given by [9]

$$L' = (W+2G)L_t\,/\,4a \tag{3}$$

where, c=3×10^8 m/s is the speed of light in free space, Z_0 and $\varepsilon_{r,eff}$ is the characteristic impedance and effective dielectric constant of the unloaded CPW t-line, respectively. And $\varepsilon_{r,eff}$ is obtained by

$$\varepsilon_{r,eff} = (\varepsilon_r + 1)/2 \tag{4}$$

where, ε_r is the relative dielectric constant of substrate. In (3), W is the width of the central conductor of CPW. G is the width of the gap between central conductor and ground plane of the CPW. a is the width of narrowed central conductor (see Fig. 1).

To avoid the MEMS switch getting connect with the CPW line when a bias voltage is applied, deposit a thin layer of insulator Si_3N_4 (the relative dielectric constant ε_i =7, the thickness t_i=0.3μm). Thus form a MIM capacitor of the MEMS bridge.

When the MEMS bridge is in the up-state position or in the down-state position, the MIM capacitance is represented by C_{bu} or C_{bd}. MIM capacitor is able to be approximated as a plate capacitor. So C_{bu} and C_{bd} are given by the following

$$C_{bu} = 1/(\frac{h}{\varepsilon_0 A_{MIM}} + \frac{t_i}{\varepsilon_0 \varepsilon_i A_{MIM}}) \tag{5}$$

and

$$C_{bd} = 1/(\frac{h_d}{\varepsilon_0 \varepsilon_i A_{MIM}} + \frac{t_i}{\varepsilon_0 \varepsilon_i A_{MIM}}) \tag{6}$$

where h and h_d are the distance between the MEMS bridge and insulator Si_3N_4 when the bridge is in the up-state and down-state position, t_i is the thickness of Si_3N_4, as shown in Fig. 1(a). ε_0=8.854×10^{-12} F/m is the dielectric constant of air, ε_i is the relative dielectric constant of Si_3N_4. And A_{MIM} is the acreage of the MIM capacitor.

As mentioned previously that metals of MAM capacitor are located on the both sides of MEMS bridge, the height of MAM capacitor is almost the same when the MEMS bridge in the down-state position comparing to that in the up-state position. And MAM capacitance can also be approximated as the capacitance of a plate capacitor, which is represented by $\frac{1}{2}C_s$.

$$\frac{1}{2}C_s = \frac{\varepsilon_0 A_{MAM}}{h+t_i} \tag{7}$$

where A_{MAM} is the acreage of the MAM capacitor.

In the unit cell, the capacitances of the MEMS switch in the up-state and down-state position are C_u and C_d, respectively. And they are the series of the MIM capacitor and MAM capacitor, as presented in Fig. 2.

$$C_u = \frac{C_s C_{bu}}{C_s + C_{bu}} \tag{8}$$

and

$$C_d = \frac{C_s C_{bd}}{C_s + C_{bd}} \tag{9}$$

In general, $C_{bu} << C_s$ and $C_{bd} >> C_s$. So, we respectively have $C_u \approx C_{bu}$ and $C_d \approx C_s$. For a *Ka*-band design, C_{bu} is around 20-50fF and C_{bd} is about 1-3pF.

Based on the above capacitance and inductance formulas, the following expressions can be solved to develop closed-form design equations for the phase shifter [11, 12].

The loaded t-line impedance Z_u (up-state position) and Z_d (down-state position) respectively are

$$Z_u = \sqrt{\frac{sL_1}{sC_t + C_u}}\sqrt{1 - \frac{\omega^2}{4}sL_1(sC_t + C_u)} \tag{10}$$

$$Z_d = \sqrt{\frac{sL_1}{sC_t + C_d}}\sqrt{1 - \frac{\omega^2}{4}sL_1(sC_t + C_d)} \tag{11}$$

where s is the spacing between each unit cell.

Then the phase shift can be determined by

$$\Delta\phi = \frac{\omega Z_0 \sqrt{\varepsilon_{r,eff}}}{c}(\frac{1}{Z_u} - \frac{1}{Z_d}) \tag{12}$$

Table 1. Unit cell parameters.

Parameters	Length [μm]
W	60
G	60
H	500
t	0.8
h	1.2
d	40
s	400
a	40
b	48

The design starts with the closed-form expressions for the phase shifter given above. For *Ka*-band, the dimensions of the unit cell of CPW t-line are chose to be 300μm×570μm×510μm, on a silicon substrate (the dielectric constant ε_r =11.9). The structural parameters of MEMS switch are listed in Table 1. The height of MEMS switch in the down-state position is h_d=0.4μm.

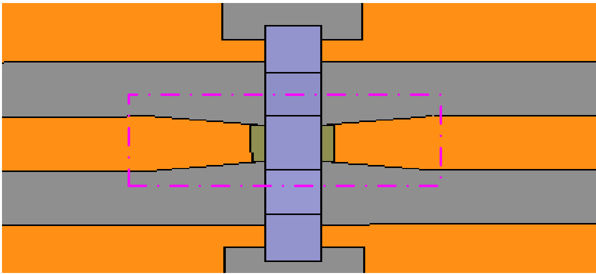

Fig. 3. Structure of the central conductor of CPW at the place where load the MEMS bridges.

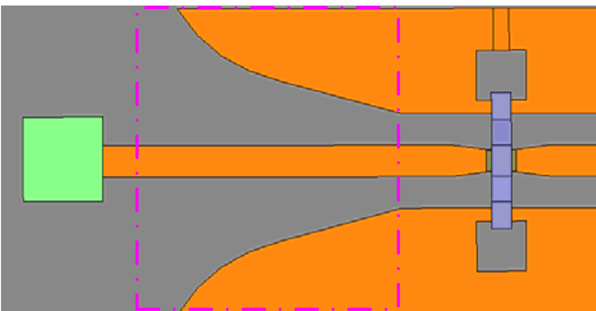

Fig. 4. Structure of the fringe of the ground plane of CPW.

As Fig. 3 shows, to counteract the transition of the impedance aroused by the capacitors, make the central conductor of CPW narrow at the place where load the MEMS bridges [9, 10].

In general, the fringes of ground planes of CPW are rectangular, which cause the signal of both ends of CPW t-line suddenly cut off. It easily forms reflection. With the increase of the bit of phase shifter, the reflection loss will be produced more. So in this design, to reduce the reflection loss, the fringes of ground planes of CPW narrow gradually as shown in Fig. 4.

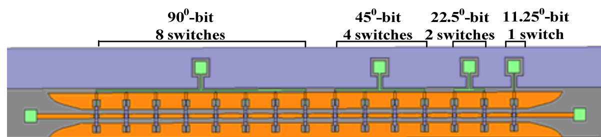

Fig. 5. 4-bit distributed MAM MEMS phase shifter.

4-Bit MAM MEMS Phase Shifter Design

Based on the analysis of unit cell, the final 4-bit MAM MEMS phase shifter is designed and simulated by Ansoft HFSS software. Fig. 5 shows the model of the 4-bit distributed MEMS Phase Shifter, which consists of 15 MEMS switches. Divide the switches into four groups with respectively 1, 2, 4 and 8 switches. According to apply bias voltage to control the switches in the up-state or down-state, they will form four basic phase of 11.25°, 22.5°, 45°, 90° and the 16 kinds of phases are constructed from them.

The dimension of 4-bit distributed MAM MEMS phase shifter is 8.40mm×11.60mm×0.51mm. The simulation results are shown in Fig. 6, 7 and 8, where Fig. 6 and 7 shows the insertion loss and reflection loss of the 4-bit phase shifter at each phase state, Fig. 8 illustrates the frequency-dependent phase shift for all 16 switching states from 25GHz to 35GHz.

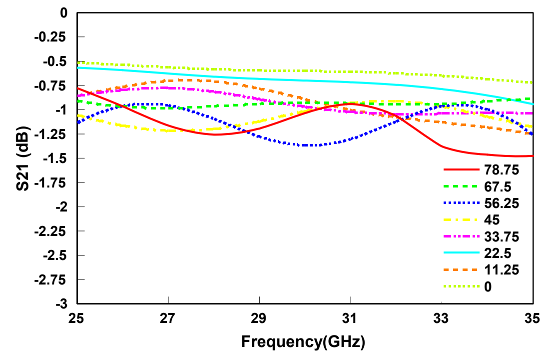

(a)

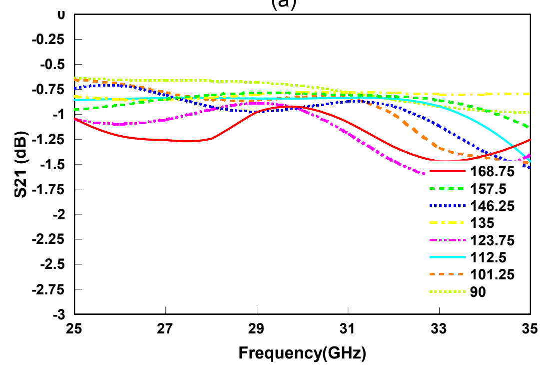

(b)

Fig. 6. Simulation results of insertion coefficient for 16 phase states. (a) Phase states of 0°-78.75°. (b) Phase states of 90°-168.75°.

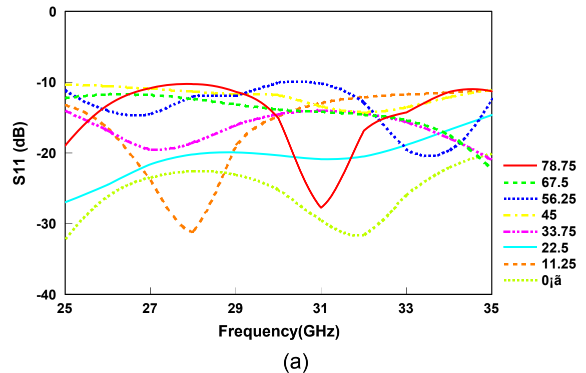

(a)

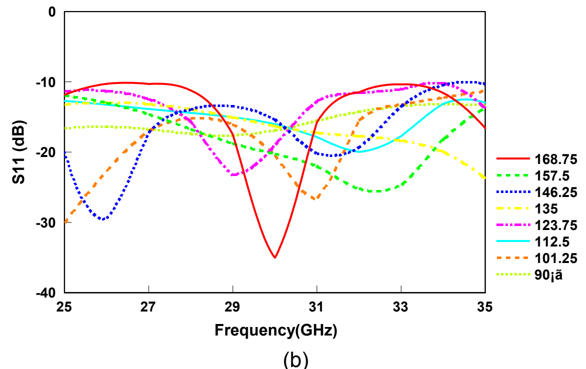

(b)

Fig. 7. Simulation results of reflection coefficient for 16 phase states. (a) Phase states of 0°-78.75°. (b) Phase states of 90°-168.75°.

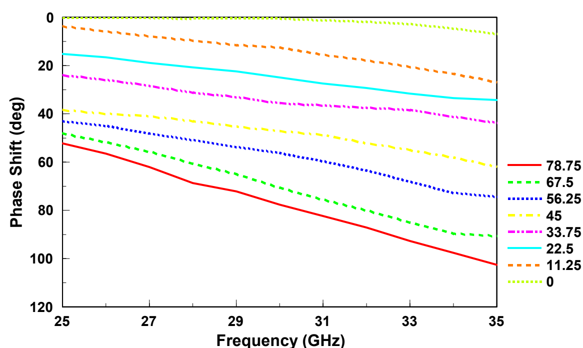

(a)

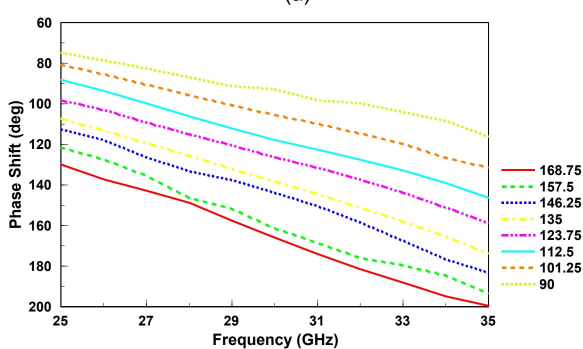

(b)

Fig. 8. Simulation results of phase shift at 30 GHz for 16 phase states. (a) Phase shift 0° -78.75°. (b) Phase shift 90° -168.75°.

Table 2. Phase shift of 4-bit MAM MEMS phase shifter at 30GHz

Phase State	Simulation	Phase Error
0°	0.26°	+0.26°
11.25°	12.278°	+1.028°
22.5°	24.917°	+2.417°
33.75°	35.223°	+1.473°
45°	46.947°	+1.947°
56.25°	56.042°	-0.208°
67.5°	70.342°	+2.758°
78.75°	77.613°	-1.137°
90°	92.567°	+2.567°
101.25°	105.233°	+3.983°
112.5°	117.857°	+5.357°
123.75°	125.908°	+2.158°
135°	138.225°	+3.225°
146.25°	143.486°	-2.764°
157.5°	160.898°	+3.398°
168.75°	165.937°	-2.813°

As shown in these figures, for all switching states, the insertion coefficient is better than -1.37dB at 30GHz, the reflection coefficient is lower than -10dB at the frequency from 25GHz to 35GHz. Besides conductive loss, the inconsistency in periodically loads of MEMS bridges and MAM capacitors will generate the phase error and deteriorate loss and matching performance. Simulation shows it will shift phase from 0° to 168.75° with 11.25° phase step at 30 GHz and the biggest error of phase is 3.983°, corresponding to an error ratio of 3.93%. Detailed phase shift data is listed in Table 2.

Conclusion

Based on MEMS technology, this paper presents a 4-bit distributed phase shifter using MAM capacitors on CPW t-line. On the basis of the unit cell analysis, a compact 4-bit phase shifter of 11.25°, 22.5°, 45°, 90° are designed. Results show that the phase shifter proposed in this paper has lower loss and high accuracy at 30 GHz. It is suitable for the applications of phase arrays.

Acknowledgments

This work was supported in part by the National Science Foundation of China and NSAF under their joint Grant 11076031.

REFERENCES

[1] Sterner M., Roxhed N., Stemme G., Oberhammer J., Static Zero-Power-Consumption Coplanar Waveguide Embedded DC-to-RF Metal-Contact MEMS Switches in Two-Port and Three-Port Configuration, *IEEE Transactions on Electron Devices*, 57(2010), No.7,1659-1669

[2] Caekenberghe K.V., Modelling RF MEMS Devices, *IEEE Microwave Magazine*, 13(2012), No.1, 83-110

[3] Persano A., Cola A., De Angelis G., Taurino A., Siciliano P., Quaranta F., Capacitive RF MEMS Switches with Tantalum-Based Materials, *Journal of Microelectromechanical Systems*, 20(2011), No.2, 365-370

[4] Zhang Q.X., Yu A. B., Rong Y., Li H.Y., Guo L.H., Liao E.B., Min T., Lo G.Q., Balasubramanian N., Kwong D.L., Integration of RF MEMS and CMOS IC on a Printed Circuit Board for a Compact RF System Application Based on Wafer Transfer, *IEEE Transactions on Electron Devices*, 55(2008), No.9, 2484-2491

[5] Reines I., S-J Park, Rebeiz G.M., Compact Low-Loss Tunable X-Band Bandstop Filter With Miniature RF-MEMS Switches, *IEEE Transactions on Microwave Theory and Techniques*, 58(2010), No.7, 1887-1895

[6] Du Y., Bao J., Zhao X., 5-bit MEMS Distributed Phase Shifter, *Electronics Letters*, 46(2010), No.21, 1452-1453

[7] Gong S.B., Shen H., Barker N.S., A 60-GHz 2-bit Switched-Line Phase Shifter Using SP4T RF-MEMS Switches, *IEEE Transactions on Microwave Theory and Techniques*, 59(2011), No.4, 894-900.

[8] Somjit N., Stemme G., Oberhammer J., Binary-Coded 4.25-bit W-Band Monocrystalline–Silicon MEMS Multistage Dielectric-Block Phase Shifters, *IEEE Transactions on Microwave Theory and Techniques*, 57(2009), No.11, 2834-2840

[9] Gupta K.C., Garg R., Bahl I., Bharia P., *Microstrip Lines and Slotlines*, 2nd edn. (Artech House, 1996), Chap.3.

[10] Rebeiz G.M., Phase-moose Analysis of MEMS-Based Circuits and Phase Shifters, *IEEE Microwave Guided Wave Letters*, 50(2002), No.5, 1316

[11] Hayden J.S., Rebeiz G.M., Very Low-loss Distributed X-band and Ka-band MEMS Phase Shifters using Metal–air–metal Capacitors, *IEEE Transactions on Microwave Theory and Techniques*, 51(2003), 309–314

[12] Topalli K., Civi O.A., Demir S., Koc S., Akin T., A Monolithic Phased Array Using 3-bit Distributed RF MEMS Phase Shifters, *IEEE Transactions on Microwave Theory and Techniques*, 56(2008), No.2, 270-277

***Authors**: Dr. Aixin CHEN, Ms. Weiwei JIANG, and Ms. Ying Li are with the School of Electronic and Information Engineering, Beihang University, Beijing 100191, China, E-mail: axchen@buaa.edu.cn, jiangweiwei@ee.buaa.edu.cn, tq03hli@163.com; Prof. Dr. Zhizhang CHEN is with the Department of Electrical and Computer Engineering, Dalhousie University, Halifax, NS B3J 2X4, Canada, E-mail: z.chen@dal.ca.*